J|A|C|S ARTICLES

Published on Web 12/02/2009

Hydrogen Exchange Rate of Tyrosine Hydroxyl Groups in Proteins As Studied by the Deuterium Isotope Effect on C_ζ Chemical Shifts

Mitsuhiro Takeda,[†] JunGoo Jee,[‡] Akira Mei Ono,[‡] Tsutomu Terauchi,[‡] and Masatsune Kainosho*,[†,‡]

Structural Biology Research Center, Graduate School of Science, Nagoya University, Furo-cho, Chikusa-ku, Nagoya, 464-8602, Japan, and Center of Priority Areas, Graduate School of Science and Technology, Tokyo Metropolitan University, 1-1 Minami-ohsawa, Hachioji, 192-0397, Japan

Received September 24, 2009; E-mail: kainosho@nmr.chem.metro-u.ac.jp

Abstract: We describe a new NMR method for monitoring the individual hydrogen exchange rates of the hydroxyl groups of tyrosine (Tyr) residues in proteins. The method utilizes (2*S*,3*R*)-[β_2,$\varepsilon_{1,2}$-$^2H_3$;0,α,β,ζ-$^{13}C_4$;^{15}N]-Tyr, ζ-SAIL Tyr, to detect and assign the $^{13}C_\zeta$ signals of Tyr rings efficiently, either by indirect ^1H-detection through 7−8 Hz $^1H_\delta-^{13}C_\zeta$ spin couplings or by direct $^{13}C_\zeta$ observation. A comparison of the $^{13}C_\zeta$ chemical shifts of three Tyr residues of an 18.2 kDa protein, EPPIb, dissolved in H_2O and D_2O, revealed that all three $^{13}C_\zeta$ signals in D_2O appeared at ∼0.13 ppm (∼20 Hz at 150.9 MHz) higher than those in H_2O. In a H_2O/D_2O (1:1) mixture, however, one of the three signals for $^{13}C_\zeta$ appeared as a single peak at the averaged chemical shifts, and the other two appeared as double peaks at exactly the same chemical shifts in H_2O and D_2O, in 50 mM phosphate buffer (pH 6.6) at 40 °C. These three peaks were assigned to Tyr-36, Tyr-120, and Tyr-30, from the lower to higher chemical shifts, respectively. The results indicate that the hydroxyl proton of Tyr-120 exchanges faster than a few milliseconds, whereas those of Tyr-30 and Tyr-36 exchange more slowly. The exchange rate of the Tyr-30 hydroxyl proton, k_{ex}, under these conditions was determined by ^{13}C NMR exchange spectroscopy (EXSY) to be 9.2 ± 1.1 s^{-1}. The Tyr-36 hydroxyl proton, however, exchanges too slowly to be determined by EXSY. These profound differences among the hydroxyl proton exchange rates are closely related to their relative solvent accessibility and the hydrogen bonds associated with the Tyr hydroxyl groups in proteins.

Introduction

In a folded, globular protein, the protons attached to the backbone and side chain nitrogen, oxygen, and sulfur atoms, even for the residues deeply buried in the interior hydrophobic core regions, are known to exchange with those of surrounding waters. Such hydrogen exchange phenomena have been ascribed to the local and/or global conformational fluctuations of proteins in solution, which expose the buried residues to the solvent. Therefore, the hydrogen exchange rates for buried residues provide crucial information about the conformational dynamics of a protein in solution.[1−11] However, most investigations have focused on the backbone amide hydrogen exchange phenomena, since the hydrogen atoms attached to the other side chain polar groups, such as hydroxyl groups, often exchange too quickly for detailed analyses, as compared to the amide hydrogen atoms.[2,4,12−14] The situation could be even more complicated for hydroxyl groups, since their hydrogen exchange rates are strongly affected by trace amounts of various contaminants, such as inorganic ions.[12,14] For instance, inorganic phosphate, which is often used in NMR buffer, acts as a catalyst that significantly increases the exchange rate of the Tyr hydroxyl protons of small peptides, even at a low phosphate concentration such as 20 mM.[14] Therefore, the conventional NMR methods developed for studying the backbone amide groups cannot successfully be applied to side chain hydroxyl groups. However, crystal structure analyses of proteins revealed that the polar groups attached to the residues in the interior of proteins not only are highly shielded from the surrounding solvent but also are often involved in the hydrogen bond networks. In these peculiar

[†] Nagoya University.
[‡] Tokyo Metropolitan University.

(1) Havdt, A.; Nielsen, S. O. *Adv. Protein Chem.* **1966**, *21*, 287–386.
(2) Englander, S. W.; Downer, N. W.; Teitelbaum, H. *Annu. Rev. Biochem.* **1972**, *41*, 903–924.
(3) Wagner, G.; Wüthrich, K. *J. Mol. Biol.* **1979**, *130*, 31–38.
(4) Woodward, C.; Simon, I.; Tuchsen, E. *Mol. Cell. Biochem.* **1982**, *48*, 135–160.
(5) Englander, S. W.; Mayne, L. *Annu. Rev. Biophys. Biomol. Struct.* **1992**, *21*, 243–265.
(6) Baldwin, R. L. *Curr. Opin. Struct. Biol.* **1993**, *3*, 84–91.
(7) Bai, Y.; Sosnick, T. R.; Mayne, L.; Englander, S. W. *Science* **1995**, *269*, 192–197.
(8) Pace, C. N.; Horn, G.; Hebert, E. J.; Bechert, J.; Shaw, K.; Urbanikova, L.; Scholtz, J. M.; Sevcik, J. *J. Mol. Biol.* **2001**, *312*, 393–404.
(9) Krishna, M. M. G.; Hoang, L.; Lin, Y.; Englander, S. W. *Methods* **2004**, *34*, 51–64.
(10) Wagner, G.; Wüthrich, K. *J. Mol. Biol.* **1979**, *134*, 75–94.
(11) Wagner, G.; Wüthrich, K. *J. Mol. Biol.* **1982**, *160*, 343–36.
(12) Englander, S. W.; Kallenbach, N. *Q. Rev. Biophys.* **1984**, *16*, 521–655.
(13) Erriksson, M. A. L.; Haerd, T.; Nilsson, L. *Biophys. J.* **1995**, *69*, 329–339.
(14) Liepinsh, E.; Otting, G. *Magn. Reson. Med.* **1996**, *35*, 30–42.

 10.1021/ja907911y

environments, the hydroxyl groups of the amino acid side chains of the buried residues might have much slower hydrogen exchange rates and could be studied without interference from trace amounts of contaminants or inorganic buffers, as compared to those of the solvent-exposed residues in peptides. Therefore, the microenvironments for the hydroxyl groups of the amino acid side chains in solution may be characterized by the detection of the slowly exchanging hydrogen atoms attached to them.

A number of NMR studies have analyzed the hydrogen exchange phenomena of side chain hydroxyl groups.[15,16] Many of the hydroxyl protons in proteins, however, were observed at the chemical shift of water, due to the fact that the chemical exchange rates between the hydroxyl and water protons are, in general, fast enough to merge their NMR signals.[17,18] Furthermore, the hydroxyl proton can hardly be detected by sensitive indirect-detection NMR measurements, such as $^{1}H-^{13}C$ correlation spectroscopy, and thus many of the hydroxyl proton signals tend to be overlooked, even though they actually appear as discrete ^{1}H NMR signals. Among the hydroxyl amino acids, i.e., Thr, Ser, and Tyr, the hydroxyl groups of Tyr residues are often involved in intermolecular hydrogen bonds within the core region of a protein.[19] Therefore, the identification and characterization of slowly exchanging Tyr hydroxyl protons is expected to provide valuable information on these auxiliary hydrogen bonds.

In addition to the direct observation of exchangeable proton signals, various alternative methods, using deuterium isotope effects on the chemical shifts of the directly or indirectly bonded carbons to study the hydrogen exchange rates for backbone amide groups, have been developed.[20−26] The deuterium substitution usually causes substantial upfield shifts for the nuclei separated by as many as three covalent bonds.[27] Thus, in a 1:1 mixture of H_2O and D_2O, for slowly exchanging amide protons, the carbonyl carbon or α-carbon signals of amide groups may appear as multiple peaks if the hydrogen−deuterium exchange rates are slower than the inverse of the respective isotope shift differences. This method was originally applied for small peptides[20,21] and then for proteins.[22−24] Simultaneous monitoring of the proton exchange rates for the amide groups of the *i*th and $(i + 1)$th residues through the two and three bond deuterium isotope effects, which can be observed for a protein dissolved in a 1:1 mixture of H_2O and D_2O, led to the development of a method to detect the correlated hydrogen exchange phenomena of a protein, which are otherwise difficult to investigate.[25]

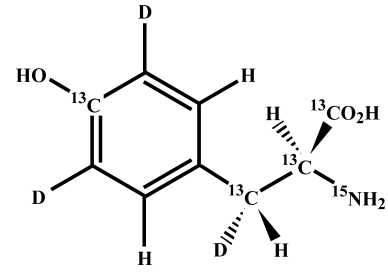

Figure 1. Stable isotope labeling pattern of SAIL (2*S*,3*R*)-[$\beta_2,\varepsilon_{1,2}$-$^{2}H_3$;0,α,$\beta$,ζ-$^{13}C_4$;^{15}N]-Tyr. ^{12}C atoms are not shown in the figure.

The deuterium isotope shift should, in principle, also be applicable for studying the hydrogen exchange rates of other polar groups of the amino acid side chains in a protein. In the case of Tyr, a sizable two-bond deuterium isotope shift is expected to be observed for the ^{13}C chemical shifts of the C_ζ atoms. Recent progress in cryogenic probe technology[28] has enabled highly sensitive, direct observations of the ^{13}C NMR spectra, even for relatively small amounts of labeled protein. However, the uniformly ^{13}C-labeled Tyr is not suitable for detecting the deuterium isotope effects of the C_ζ NMR signals, since the $^{13}C-^{13}C$ spin couplings between $^{1}J(^{13}C_\zeta-^{13}C_{\varepsilon 1/2})$, ∼70 Hz, and $^{3}J(^{13}C_\zeta-^{13}C_\gamma)$, ∼10 Hz, result in complex, broad signals.[29] The lack of robust assignment methods for the $^{13}C_\zeta$ signals has further limited the use of the uniformly ^{13}C-labeled Tyr. In the present study, we describe a new method to observe and assign the $^{13}C_\zeta$ signals of the Tyr rings in a protein and to investigate the hydrogen exchange rates of individual hydroxyl groups of Tyr residues, by observing the two-bond deuterium isotope shift, $^{2}\Delta\delta^{13}C_\zeta$, for the $^{13}C_\zeta$ signals. In doing so, we synthesized a new type of stereoarray isotope labeled (SAIL) amino acid,[30] (2*S*,3*R*)-[$\beta_2,\varepsilon_{1,2}$-$^{2}H_3$;0,α,$\beta$,ζ-$^{13}C_4$;^{15}N]-Tyr, ζ-SAIL Tyr, which has the optimal isotope-labeling pattern for the present purpose (Figure 1). We used an *E. coli* cell-free protein expression system to incorporate ζ-SAIL Tyr into an 18.2 kDa *E. coli* protein, peptidyl-prolyl *cis-trans* isomerase b (EPPIb), for which we had already established the sequential assignment[31] and determined the solution structure.[32] By virtue of the optimal labeling pattern of the ζ-SAIL Tyr residues, the three $^{13}C_\zeta$ atoms of the Tyr residues in EPPIb were readily assigned and then used for studying the hydrogen exchange rates of the Tyr hydroxyl groups.

Materials and Methods

(2*S*,3*R*)-[$\beta_2,\varepsilon_{1,2}$-$^{2}H_3$;0,α,$\beta$,ζ-$^{13}C_4$;^{15}N]-Tyr, ζ-SAIL Tyr (6). ζ-SAIL Tyr **6** was synthesized according to the scheme described in Figure 2. The [4-^{13}C]4*H*-pyran-4-one **2** was derived from [2-^{13}C]-acetone (CIL) **1** by the method described previously, with slight modifications.[33,34] Treatment of **2** with diethyl [1,3-$^{13}C_2$]-malonate (CIL) in the

(15) Liepinsh, E.; Otting, G.; Wüthrich, K. *J. Biomol. NMR* **1992**, *2*, 447–465.
(16) Pfeiffer, S.; Spitzner, N.; Löhr, F.; Rüterjans, H. *J. Biomol. NMR* **1998**, *11*, 1–15.
(17) Otting, G.; Wüthrich, K. *J. Am. Chem. Soc.* **1989**, *111*, 1871–1875.
(18) Otting, G.; Liepinsh, E.; Wüthrich, K. *J. Am. Chem. Soc.* **1991**, *113*, 4363–4364.
(19) Pace, C. N.; Horn, G.; Hebert, E. J.; Bechert, J.; Shaw, K.; Urbanikova, L.; Scholtz, J. M.; Sevcik, J. *J. Mol. Biol.* **2001**, *312*, 393–404.
(20) Feeney, J.; Partington, P.; Roberts, G. C. K. *J. Magn. Reson.* **1974**, *13*, 268–274.
(21) Hawkes, G. E.; Randall, E. W.; Hull, W. E.; Gattegno, D.; Conti, F. *Biochemistry* **1978**, *17*, 3986–3993.
(22) Kainosho, M.; Tsuji, T. *Biochemistry* **1982**, *21*, 6273–6279.
(23) Kainosho, M.; Nagao, H.; Tsuji, T. *Biochemistry* **1987**, *26*, 1068–1075.
(24) Markley, J. L.; Kainosho, M. In *Stable Isotope Labeling and Resonance Assignments in Larger Proteins: NMR of Macromolecules*; Roberts, G. C. K., Ed.; Oxford University Press: New York, 1993; pp 101−152.
(25) Uchida, K.; Markley, J. L.; Kainosho, M. *Biochemistry* **2005**, *44*, 11811–11820.
(26) Liu, A.; Lu, Z.; Wang, J.; Yao, L.; Li, Y.; Yan, H. *J. Am. Chem. Soc.* **2008**, *130*, 2428–2429.
(27) Hansen, P. E. *Annu. Rep. NMR Spectrosc.* **1983**, *15*, 105–234.
(28) Serber, Z.; Richter, C.; Dötsch, V. *ChemBioChem* **2001**, *2*, 247–251.
(29) Torizawa, T.; Ono, A. M.; Terauchi, T.; Kainosho, M. *J. Am. Chem. Soc.* **2005**, *127*, 12620–12626.
(30) Kainosho, M.; Torizawa, T.; Iwashita, Y.; Terauchi, T.; Ono, A. M.; Güntert, P. *Nature* **2006**, *440*, 52–57.
(31) Kariya, E.; Ohki, S.; Hayano, T.; Kainosho, M. *J. Biomol. NMR.* **2000**, *18*, 75–76.
(32) Takeda, M.; Terauchi, T.; Ono, A. M.; Kainosho, M. *J. Biomol. NMR* **2009**, in press; DOI: 10.1007/s10858-009-9360-9.
(33) Riegel, E. R.; Zwilgmeyer, F. *Organic Synthesis*; Wiley: New York, 1943 *Collect. Vol.* 2, p 126.
(34) Owen, G. E., Jr.; Pearson, J. M.; Szwarc, M. *Trans. Faraday. Soc.* **1964**, *60*, 564–571.

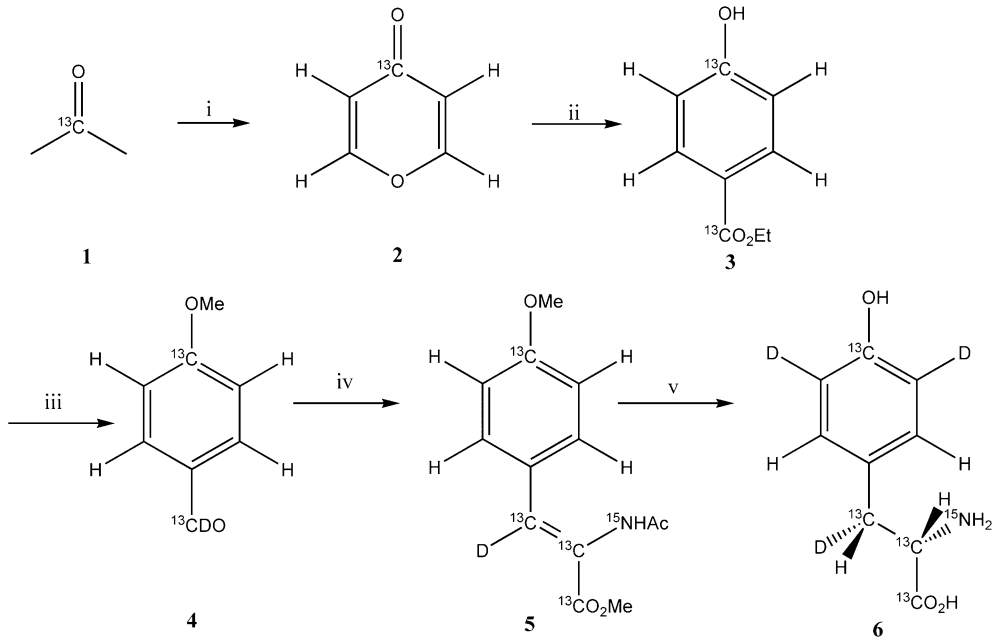

Reagents and conditions: (i) (1) $(EtO_2C)_2$, EtONa/EtOH, (2) concHCl, (3) Cu ; (ii) Ethyl [1,3-$^{13}C_2$]-Malonate, *t*-BuOK ; (iii) (1) MeI / Acetone, (2) $LiAlD_4$, (3) MnO_2; (iv) (1) NAc-[$^{13}C_2$;^{15}N]-glycine, Ac_2O, AcONa, (2) MeOH, Et_3N; (v) (1) (*S*,*S*)-Et-DuPhos-Rh, H_2, (2) 1N-HCl, (3) HBr-H_2O, (4) 6N-DCl

Figure 2. Synthesis scheme for (2*S*,3*R*)-[β_2,$\varepsilon_{1,2}$-$^2H_3$;0,α,β,ζ-$^{13}C_4$;^{15}N]-Tyr, ζ-SAIL Tyr.

presence of *tert*-butoxide afforded the ethyl hydroxybenzoate **3**.[35] After methylating the hydroxyl group of **3**, the ester was reduced by $LiAlH_4$ and then oxidized by MnO_2 to give the anisaldehyde **4**. Then, **4** was converted into the dehydrotyrosine derivative **5** by condensation with *N*-acetyl [$^{13}C_2$,^{15}N]-Gly. The intermediate **5** in methanol was hydrogenated in the presence of (*S*,*S*)-EtDuPhos-Rh (Sigma-Aldrich) as a catalyst. After deprotection under acidic conditions, the resulting labeled Tyr was converted into (2*S*,3*R*)-[β_2,$\varepsilon_{1,2}$-$^2H_3$;0,α,β,ζ-$^{13}C_4$;^{15}N]-Tyr, ζ-SAIL Tyr, **6**, by refluxing in 6 N DCl/D_2O overnight.[36]

Cell-Free Expression of *E. coli* Peptidyl-prolyl *cis-trans* Isomerase b, EPPIb, Selectively Labeled with ζ-SAIL Tyr. The EPPIb selectively labeled with ζ-SAIL Tyr was prepared by an *E. coli* cell-free system, as described previously.[37,38] According to the protocol, 5 mL of the reaction mixture containing the cell extract from *E. coli* BL21 Star (DE3) (Invitrogen) and all other components were placed in a dialysis tube and dialyzed against 20 mL of outer medium for 8 h. The concentration of ζ-SAIL Tyr was 0.5 mM, and that of each of the other 19 unlabeled amino acids was 1 mM for both the inner and outer solutions. After purification according to the previously reported method,[31] NMR samples containing 0.5 mM EPPIb, in 50 mM sodium phosphate, pH 6.6, 100 mM NaCl and 0.1 mM NaN_3, were obtained by a single cell-free expression step.

NMR Measurements. All NMR experiments were performed on a DRX600 spectrometer (Bruker Biospin; 600.3 MHz for ^1H) equipped with a TCI cryogenic triple resonance probe at 40 °C for 0.5 mM, pH 6.6 (uncorrected) ζ-SAIL Tyr labeled EPPIb solutions, unless stated otherwise. The $^1H-^{13}C$ constant-time HSQC (ct-HSQC) spectrum for the aliphatic region was obtained for the EPPIb sample in 100% D_2O. The data size and spectral width were 256 (t_1) × 1024 (t_2) and 6000 Hz (ω_1, ^{13}C) × 8000 Hz (ω_2, ^1H), respectively. The carrier frequencies of ^{13}C and ^1H were 45 and 4.7 ppm, respectively. The ^2H decoupling was applied during t_1 chemical shift encoding. The ^{13}C-edited NOESY-HSQC experiments were performed with a data size of 200 (t_1) × 32 (t_2) × 1024 (t_3) and a spectral width of 6600 Hz (ω_1, ^1H) × 3000 Hz (ω_2, ^{13}C) × 6600 Hz (ω_3 ^1H). The carrier frequencies of ^1H and ^{13}C were 4.7 and 40 ppm, respectively. The $^1H-^{13}C$ HSQC spectra of the aromatic region were acquired in 100% D_2O (Figure 3D) and in 50% D_2O/50% H_2O (Figure 4D). In the INEPT elements composed of $[(\pi/2)_x(^1H)$-τ-$\pi(^1H,^{13}C)$-τ-$(\pi/2)_y(^1H)]$, the delay τ was 12.5 ms. The data size and the spectral width were 256 (t_1) × 1024 (t_2) and 3000 (ω_1, ^{13}C) Hz and 8000 Hz (ω_2, ^1H), respectively. The carrier frequencies were 158 ppm for ^{13}C and 4.7 ppm for ^1H.

The ^{13}C direct observations of EPPIb labeled with ζ-SAIL Tyr in different H_2O/D_2O ratios were performed with proton decoupling by a WALTZ16 ^1H decoupling scheme.[39] The carrier frequency of carbon was set to 157 ppm, and the sweep width was 4500 Hz. The repetition time was 3 s. In the case of the sample in 100% H_2O, a 4.1 mm o.d. Shigemi tube containing the protein solution was inserted into a 5 mm o.d. outer tube containing D_2O for the ^2H lock signal.

The ^{13}C NMR EXSY experiments were accomplished by using 0.7 mM EPPIb selectively labeled with ζ-SAIL Tyr in a mixture of 50% H_2O and 50% D_2O. The pulse scheme used for the experiment was basically identical to that in the previously reported $^{13}C-^{13}C$ NOE experiment.[40,41] During the chemical shift encoding (t_1) and the acquisition of free induction decay (t_2), decoupling on ^1H by the WALTZ16 scheme was applied.[39] The spectra were acquired for two different spectral regions. In the first set, the data points and spectral widths were 256 (t_1) × 1024 (t_2) points and 1500 Hz (ω_1, ^{13}C) × 2300 Hz (ω_2, ^{13}C), respectively, and the

(35) Lang, M.; Lang-Fugmann, S.; Steglich, W. *Organic Syntheses*; Wiley: New York, 2002; *Collect. Vol. 78*, pp 113−122.
(36) Rittenberg, D.; Keston, A. S.; Schoenheimer, R.; Foster, G. L. *J. Biol. Chem.* **1938**, *125*, 1–12.
(37) Torizawa, T.; Shimizu, M.; Taoka, M.; Miyano, H.; Kainosho, M. *J. Biomol. NMR* **2004**, *30*, 311–325.
(38) Takeda, M.; Ikeya, T.; Güntert, P.; Kainosho, M. *Nat. Protoc.* **2007**, *2*, 2896–2902.
(39) Shaka, A. J.; Keeler, J.; Frenkiel, T.; Freeman, R. *J. Magn. Reson.* **1969**, *52*, 335–338.
(40) Fischer, M. W. F.; Zeng, L.; Zuiderweg, E. R. P. *J. Am. Chem. Soc.* **1996**, *118*, 12457–12458.
(41) Bertini, I.; Felli, I. C.; Kümmerle, R.; Moskau, D.; Pierattelli, R. *J. Am. Chem. Soc.* **2004**, *126*, 464–465.

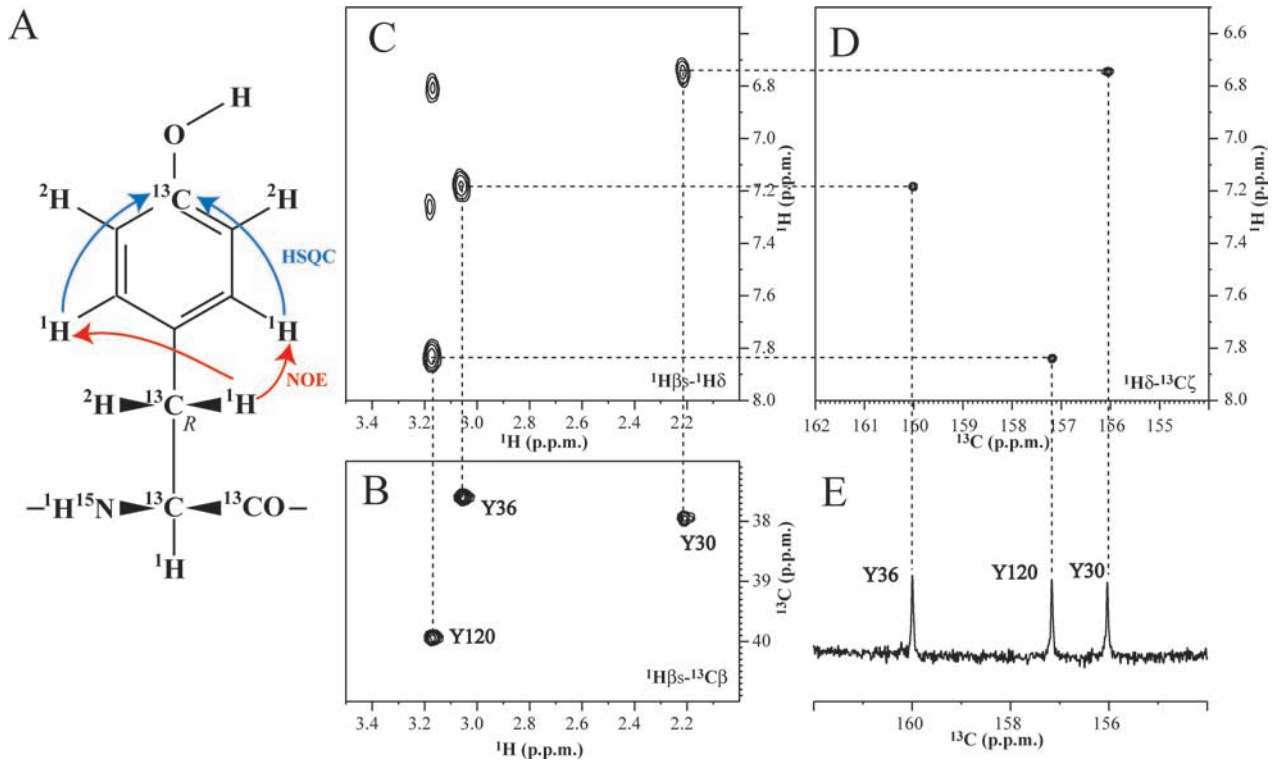

Figure 3. Assignment of the $^{13}C_\zeta$ peaks in the ζ-SAIL Tyr. (A) Magnetization transfer pathways for the assignment of the $^{13}C_\zeta$ peak. (B−E) NMR spectra of 0.5 mM of EPPIb residue-selectively labeled by ζ-SAIL Tyr under conditions of 100% D_2O at 40 °C, using a DRX600 spectrometer equipped with a TCI cryogenic probe (Bruker). (B) $^1H-^{13}C$ constant-time HSQC spectrum. ^2H decoupling was applied during t_1 chemical shift encoding. The peaks are labeled with their assignments. (C) ^{13}C-edited NOESY-HSQC spectrum. This spectrum represents an overlay of three strips at the $^{13}C_\beta$ chemical shifts of Tyr-30, Tyr-36, and Tyr-120. The intra-residue NOE establishes the connection between the $H_{\beta s}$ and H_δ resonances. (D) $^1H-^{13}C$ HSQC spectrum. The observed peaks correspond to the correlations via long-range coupling between $^1H_\delta$ and $^{13}C_\zeta$. (E) ^1H decoupled ^{13}C NMR spectrum. The $^{13}C_\zeta$ peaks are labeled with their assignments.

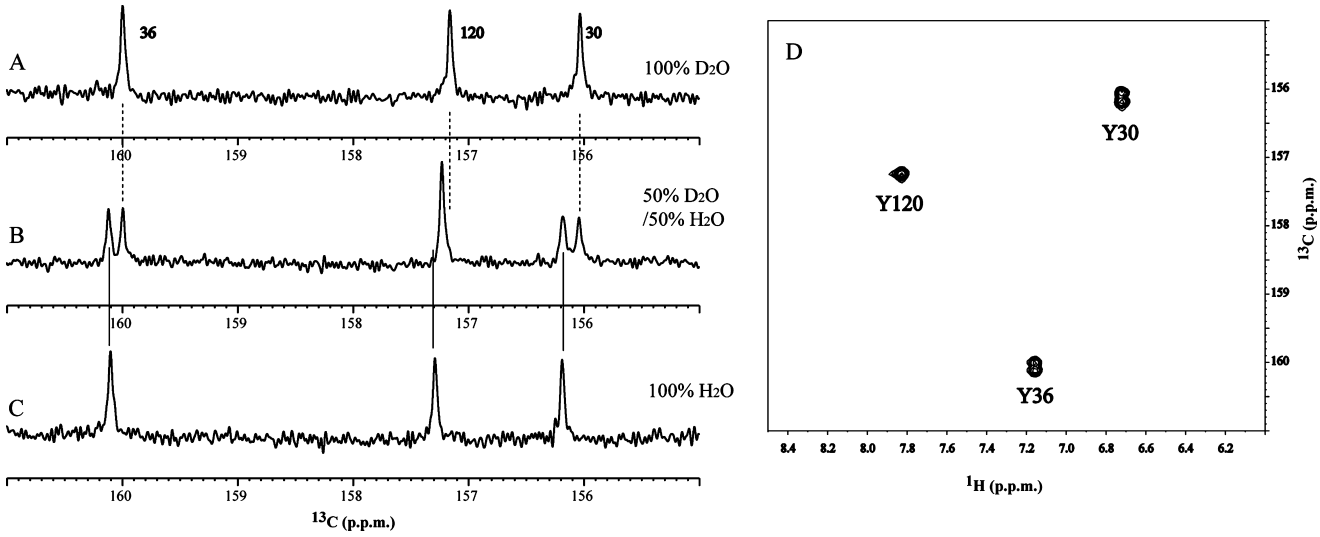

Figure 4. Observation of the deuterium isotope effect on the $^{13}C_\zeta$ peaks. (A−C) Proton-decoupled ^{13}C NMR spectra of EPPIb selectively labeled with ζ-SAIL Tyr under conditions of 100% D_2O (A), 50% H_2O/50% D_2O (B), and 100% H_2O (C). The peaks are labeled with the residue numbers in spectra A. To clarify the deuterium-induced isotope shift, solid and dashed lines are indicated for the peak positions of protonated and deuterated species, respectively. These spectra were acquired in 50 mM phosphate buffer (pH 6.6) at 40 °C by using a DRX600 spectrometer (Bruker). (D) $^1H-^{13}C$ HSQC of EPPIb labeled by ζ-SAIL Tyr in 50% H_2O/50% D_2O. The peak doubling of the $^{13}C_\zeta$ peaks for Tyr-30 and Tyr-36 in a mixture of H_2O and D_2O can also be observed by indirect ^1H-detection through $^1H_\delta-^{13}C_\zeta$ spin couplings, as shown in panel D.

number of scans/FID was 64. The carrier frequency of carbon was set to 157 ppm. The mixing times were 25, 100, and 400 ms, and the repetition time was 3.5 s. In the second set, the data points and spectral widths were 32 (t_1) × 1024 (t_2) points and 1500 Hz (ω_1, ^{13}C) × 2300 Hz (ω_2,^{13}C), respectively. The number of scans/FID was 400. The carrier frequency of carbon was 156 ppm, representing the $^{13}C_\zeta$ chemical shift of Tyr-30. The repetition time was 3.5 s. The mixing times were 0, 25, 50, 100, 200, 300, 400, and 600 ms, and the data were acquired in an interleaved manner. The second data set of the ^{13}C NMR EXSY was used for the kinetic analysis

of the Tyr-30 hydroxyl proton exchange rate. Data processing and peak picking were accomplished with NMRPipe.[42] We used the baseline noise level as the uncertainty in each experiment. At time t, the change in peak intensities between sites a and b can be expressed as 1, according to McConnell's equations.[43]

$$\frac{\mathrm{d}}{\mathrm{d}t}\begin{pmatrix} I^{\mathrm{HH}} \\ I^{\mathrm{HD}} \end{pmatrix} = \begin{pmatrix} -R^{\mathrm{H}} - k_{\mathrm{ex}} \cdot p_{\mathrm{D}} & k_{\mathrm{ex}} \cdot p_{\mathrm{H}} \\ k_{\mathrm{ex}} \cdot p_{\mathrm{D}} & -R^{\mathrm{D}} - k_{\mathrm{ex}} \cdot p_{\mathrm{H}} \end{pmatrix} \begin{pmatrix} I^{\mathrm{HH}} \\ I^{\mathrm{HD}} \end{pmatrix} \quad (1)$$

Here I^{HH} and I^{HD} mean the intensities of the auto and cross peaks, respectively. When the populations for a and b are p_{H} and p_{D} ($p_{\mathrm{H}} + p_{\mathrm{D}} = 1$), the exchange rates from H $\rightarrow$ D and D $\rightarrow$ H are expressed as k_{HD} and k_{DH} and further as $k_{\mathrm{ex}} \cdot p_{\mathrm{D}}$ and $k_{\mathrm{ex}} \cdot p_{\mathrm{H}}$ ($k_{\mathrm{HD}} + k_{\mathrm{DH}} = k_{\mathrm{ex}}$), respectively. $R^{\mathrm{H,D}}$ means the signal decay rate during the delay. In our system, eq 1 can be further simplified into eq 2 under the following assumptions: $p_{\mathrm{H}} = p_{\mathrm{D}} = 0.5$ and $R^{\mathrm{H}} = R^{\mathrm{D}} = R$.

$$\frac{\mathrm{d}}{\mathrm{d}t}\begin{pmatrix} I^{\mathrm{HH}} \\ I^{\mathrm{HD}} \end{pmatrix} = \begin{pmatrix} -R - 0.5k_{\mathrm{ex}} & 0.5k_{\mathrm{ex}} \\ 0.5k_{\mathrm{ex}} & -R - 0.5k_{\mathrm{ex}} \end{pmatrix} \begin{pmatrix} I^{\mathrm{HH}} \\ I^{\mathrm{HD}} \end{pmatrix} \quad (2)$$

With eqs 1 and 2, all four peaks, I^{HH}, I^{HD}, I^{DD}, and I^{DH}, were simultaneously fitted. Since there is no significant improvement in the statistical F-test ($P = 0.01$) for eq 1 within the current uncertainties, we chose the parameters in eq 2 as the final results. The reduced χ^2 value for eq 2 was 0.56. For the error analysis, 500 cycles of Monte Carlo simulation were tried. All of the fittings and analyses were performed using MATLAB (The MathWorks, Inc., MA). The upper limit of the Tyr-36 hydroxyl exchange rate was estimated using the equations for a two-site exchange process[44] with the following assumptions: (i) The intensities of an exchange peak at a mixing time of 400 ms are less than 10% of that of an auto peak. (ii) The proton fractionation factor is unity. (iii) The longitudinal relaxation rates of $^{13}C_\zeta$ atoms linked to OH and OD are identical.

The searches for NOE peaks involving the hydroxyl protons of Tyr-30 and Tyr-36 were performed for NOESY spectra obtained from EPPIb samples composed of 20 SAIL amino acids with different isotope labeling patterns of the phenylalanine and tyrosine residues.[32]

Results and Discussion

$^{13}C_\zeta$ Isotope Shift Measurements for Tyr Residues Induced by the Deuteration of Hydroxyl Groups. The two-bond deuterium induced isotope shifts of Tyr $^{13}C_\zeta$, $^2\Delta\delta^{13}C_\zeta$, can be accurately observed by either direct ^{13}C NMR observation or indirect ^{1}H-detection through 7−8 Hz $^1H_\delta$-$^{13}C_\zeta$ spin couplings. The $^1H_\delta$ atoms can be assigned via their NOE correlations with the H_β atoms. Based on this idea, we synthesized ζ-SAIL Tyr, in which the C_ζ atom is enriched with ^{13}C and the two H_ε protons are substituted by ^2H (Figures 1, 2). We then incorporated ζ-SAIL Tyr into an 18.2 kDa *E. coli* peptidyl-prolyl *cis*−*trans* isomerase b (EPPIb), which contains three Tyr residues (Tyr-30, Tyr-36 and Tyr-120), by using the *E. coli* cell-free system.[37,38]

Assignment of $^{13}C_\zeta$ Resonances in Tyr Rings. The assignment strategy of the $^{13}C_\zeta$ resonances is shown in Figure 3A. In ζ-SAIL Tyr, the $^1H_{\beta s}$ atom is stereospecifically substituted by deuterium, which drastically improves the quality of the $^1H-^{13}C$ correlation spectra[30] (Figure 3B). The $^1H_{\beta s}$ resonances could readily be connected to the $^1H_\delta$ peaks via the intra-residue NOE (Figure 3C). Subsequently, the H_δ resonances were correlated with the $^{13}C_\zeta$ resonances via the 7−8 Hz three-bond scalar couplings (Figure 3D). Since the $^{13}C_\zeta$ atom is free from strong one-bond scalar coupling and dipolar interactions, it yields a sharp peak on the ^{13}C NMR spectrum (Figure 3E).

Identification of Slowly Exchanging Tyr Hydroxyl Groups. As the next step, we observed EPPIb labeled with ζ-SAIL Tyr under different H_2O/D_2O conditions. In a 100% H_2O solution in 50 mM phosphate buffer (pH 6.6) at 40 °C, the three $^{13}C_\zeta$ peaks of Tyr-30, Tyr-36 and Tyr-120 were observed at 156.2, 160.1, and 157.3 ppm, respectively (Figure 4C). At a carbon resonance frequency of 150.9 MHz, the line widths of the $^{13}C_\zeta$ peaks were around 8 Hz. It should be noted that the line widths of the Tyr C_ζ signals were significantly narrower than those of the backbone carbonyl carbon signals of this protein. For example, in the spectrum for EPPIb selectively labeled with [1-^{13}C]-Ala, the line widths of the Ala carbonyls were found to be about 13 Hz under the same conditions (data not shown). In a 100% D_2O solution, all three $^{13}C_\zeta$ signals in D_2O appeared at about 0.13 ppm (ca. 20 Hz at 150.9 MHz for ^{13}C) higher than those in H_2O, corresponding to the expected deuterium-induced isotope shift (Figure 4A). In a 1:1 mixture of H_2O and D_2O, the $^{13}C_\zeta$ atoms of Tyr-30 and Tyr-36 were observed as double peaks, each resonating at exactly the same chemical shift in 100% ^1H_2O and 100% D_2O, respectively. In contrast, the $^{13}C_\zeta$ peak of Tyr-120 was observed as a single line at the averaged chemical shift (Figure 4B). This result shows that the lifetimes of the hydroxyl proton are longer than the inverse of $^2\Delta^{13}C_\zeta$ (D) in the Hz scale for Tyr-30 and Tyr-36, whereas that of Tyr-120 is shorter. The peak doubling for Tyr-30 and Tyr-36 could also be observed by indirect ^{1}H-detection through the $^1H_\delta-^{13}C_\zeta$ spin couplings (Figure 4D).

To quantitatively estimate the hydroxyl proton exchange rates of Tyr-30 and Tyr-36, ^{13}C NMR exchange spectroscopy (EXSY) experiments were used. In these experiments, the exchange between OH and OD is observed as an exchange peak. In principle, the employed pulse scheme was identical to that of $^{13}C-^{13}C$ NOESY.[40,41] The spin system of ζ-SAIL Tyr has been designed to ensure that the observable cross peaks exclusively originate from chemical exchange between protonated and deuterated species, as a result of the complete absence of dipole interactions. With increasing mixing times, the exchange-peak appeared for the Tyr-30 residue, but not for the Tyr-36 residue, over a range of 25−400 ms (Figure 5A). Based on the relative peak intensities of the exchange and auto peaks, the H/D exchange rate, $k_{\mathrm{ex}} = k_{\mathrm{HD}} + k_{\mathrm{DH}}$, for Tyr-30 OH at 40 °C was estimated to be $9.2 \pm 1.1\ \mathrm{s}^{-1}$ (Figure 5B). On the other hand, the hydrogen exchange rate, $k_{\mathrm{ex}} = k_{\mathrm{HD}} + k_{\mathrm{DH}}$, of Tyr-36 OH is much slower than $\sim 0.5\ \mathrm{s}^{-1}$, assuming that the intensity of the cross peak is smaller than 10% of the diagonal peak at a mixing time of 400 ms.

Observation and Assignment of ^{1}H Signals for the Slowly Exchanging Tyr Hydroxyl Protons. Because the lifetimes of the hydroxyl protons of Tyr-30 and Tyr-36 are relatively long, these protons might be shielded from the surrounding water or even involved in the intramolecular hydrogen bonds. In fact, the crystal structure of EPPIb (PDB code 2NUL)[45] indicates that the hydroxyl oxygen atoms of Tyr-30 and Tyr-36 are highly shielded from the solvent (see Table 1). We also searched for the proximate atoms that can be involved in hydrogen bonds

(42) Delaglio, F.; Grzesiek, S.; Vuister, G. W.; Zhu, G.; Pfeifer, J.; Bax, A. *J. Biomol. NMR* **1995**, *6*, 277–293.
(43) McConnell, H. M. *J. Chem. Phys.* **1958**, *28*, 430–431.
(44) Palmer, A. G., 3rd; Kroenke, C. D.; Loria, J. P. *Methods Enzymol.* **2001**, *339*, 204–238.
(45) Edwards, K. J.; Ollis, D. L.; Dixon, N. E. *J. Mol. Biol.* **1997**, *271*, 258–265.

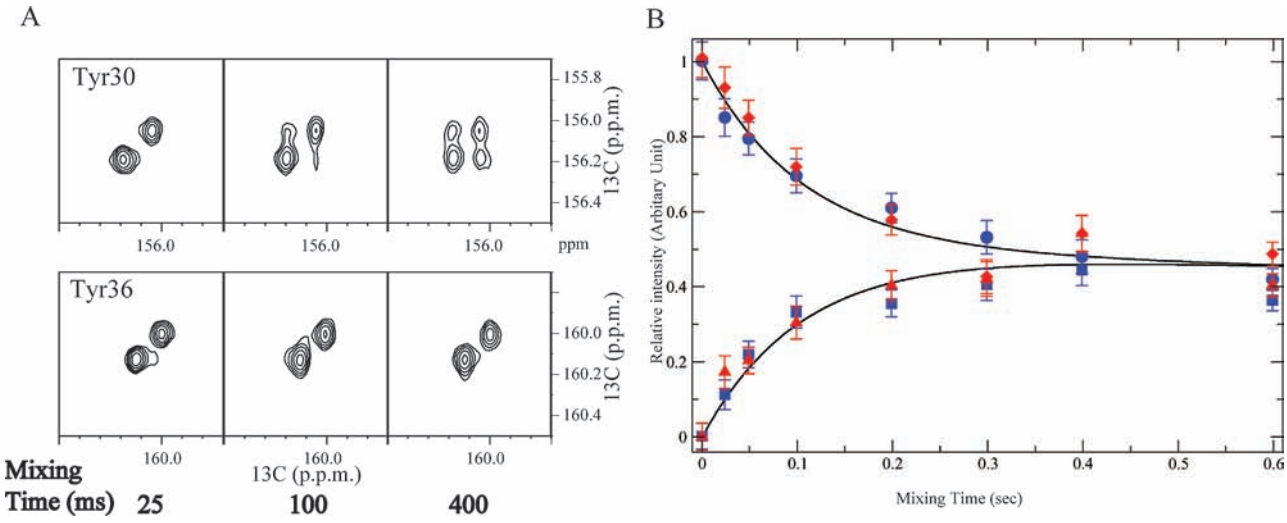

Figure 5. ^{13}C-EXSY experiments. (A) Spectral regions showing auto and exchange peaks of Tyr-30 and Tyr-36 in the ^{13}C-EXSY experiments at mixing times of 25, 100, and 400 ms. A 0.7 mM concentration of EPPIb selectively labeled with ζ-SAIL Tyr in a H_2O/D_2O (1:1) solution at 40 °C was used. (B) Amplitudes of the diagonal and cross peaks as a function of mixing time in ^{13}C-EXSY for the Tyr-30 $^{13}C_\zeta$ peaks. Diagonal peaks (■, ▲) and cross peaks (●, ◆) are plotted as a function of mixing time. The curve fitting was accomplished with MATLAB (The MathWorks, Inc., Natick, MA, USA).

Table 1. Summary of Individual Hydroxyl Hydrogen Exchange Rates in EPPIb in 50 mM Phosphate Buffer (pH 6.6) at 40 °C

amino acid residue	k_{ex} (s^{-1})	relative solvent accessibility (%)[a]
Tyr-30	9.2 ± 1.1	0
Tyr-36	<0.5	2.3
Tyr-120	>100	92.5

[a] Relative solvent accessibility was calculated on the basis of the X-ray coordinates of EPPIb at 2.1 Å resolution (PDB code 2NUL), with the use of the MolMol software.[55] The calculations were performed for the hydroxyl oxygen atom in each Tyr residue.

with these hydroxyl groups. In the case of Tyr-36, the carboxyl oxygen atom of Ala-96 resides within 3.5 Å of the hydroxyl oxygen atom, indicating hydrogen bond formation between the hydroxyl proton of Tyr-36. By virtue of the slow exchange rate of the Tyr-36 hydroxyl proton, we could actually identify a discrete ^{1}H signal for the hydroxyl group of Tyr-36, through the intra-residue NOE between the hydroxyl and ε-ring protons, using the EPPIb sample labeled with (2*S*,3*R*)-[β_2,$\delta_{1,2}$-$^2H_3$;0,α,β,γ,$\varepsilon_{1,2}$-$^{13}C_6$;^{15}N]-Tyr, ε-SAIL Tyr.[29,32] After establishing the Tyr-36 hydroxyl proton peak assignment, a number of inter-residue NOEs involving it were also identified, which allowed us to define the orientation of the hydroxyl group of Tyr-36 very precisely (Figure 6A) (see Supporting Information). In the case of Tyr-30, the oxygen atom of the hydrated water molecule is found in the crystal structure as a potential hydrogen acceptor within 3.5 Å of its hydroxyl oxygen atom (Figure 6B). In our NOESY experiment, however, we could find only two NOEs for the hydroxyl proton of Tyr-30, namely, an intra-residue NOE with ^{1}Hε and an inter-residue NOE with the backbone amide proton of Lys-65, and thus we could not precisely determine the orientation of the O−H bond. Considering the fact that this region is near the molecular surface and the hydrated water molecule presumably exchanges rapidly with the solvent water, conformational fluctuations may occur around this region, possibly leading to the faster hydroxyl proton exchange rate of Tyr-30 compared with that of Tyr-36, which is embedded in the hydrophobic core of the protein.

It is important to notice that such slowly exchanging hydroxyl proton peaks, as observed for Tyr-30 and Tyr-36 in EPPIb, might be overlooked or misinterpreted by conventional NMR spectral analyses. Especially, in the case of a protein complexed with ligands, the *intra*-molecular NOE peaks associated with the slowly exchanging hydroxyl proton signals might be misinterpreted as *inter*-molecular NOEs, since such hydroxyl proton signals cannot be purged by the ^{13}C- or ^{15}N-filtered experiments. Therefore, it would be very useful to identify the slowly exchanging hydroxyl protons of amino acid residues, using the straightforward method described herein, to avoid possible misinterpretations of NOE signals. The question arises as to whether the hydroxyl proton peak is necessarily observable for the slowly exchanging hydroxyl groups determined through the $^{13}C_\zeta$ observation. According to the NMR database (BioMagResBank, http://www.bmrb.wisc.edu/), the mean chemical shift value of the Tyr hydroxyl proton peak is 9.3 ppm, with a standard deviation of 1.4 ppm. Thus, the chemical shift difference between most hydroxyl proton peaks and water peaks is on the order of 10^3 Hz. In contrast, the chemical shift difference between two $^{13}C_\zeta$ peaks linked to OH and OD species is on the order of 10 s^{-1}, which is 2 orders of magnitude slower than the upper limits for the detection of the hydroxyl proton peak. It is thus expected that the hydroxyl proton peak would almost always appear as a discrete ^{1}H NMR signal, when the $^{13}C_\zeta$ peak is observed as a doublet in the H_2O/D_2O mixture, as in the cases of Tyr-30 and Tyr-36 of EPPIb. Therefore, once the slowly exchanging hydroxyl groups are identified by the $^{13}C_\zeta$ observation, ε-SAIL Tyr can be used to identify the corresponding hydroxyl proton peak through NOEs with Hε. On the other hand, this consideration also suggests that the hydroxyl proton peak is observable, even though the $^{13}C_\zeta$ gives a single averaged peak, at an exchange rate on the order of 10^2-10^3 s^{-1} (see Supporting Information). We recommend checking for the presence of discrete ^{1}H NMR signals of the hydroxyl proton peak through NOEs with the Hε proton for all Tyr residues, by using protein samples labeled by ε-SAIL Tyr. It is useful to remember that the hydroxyl proton peak is expected to be broad as a result of chemical exchange relaxation at the exchange rate of 10^2-10^3 s^{-1}. According to previous reports, the size of the line-broadening is $\Delta_{obs} - \Delta_{nat} = k/\pi$, where Δ_{obs} and

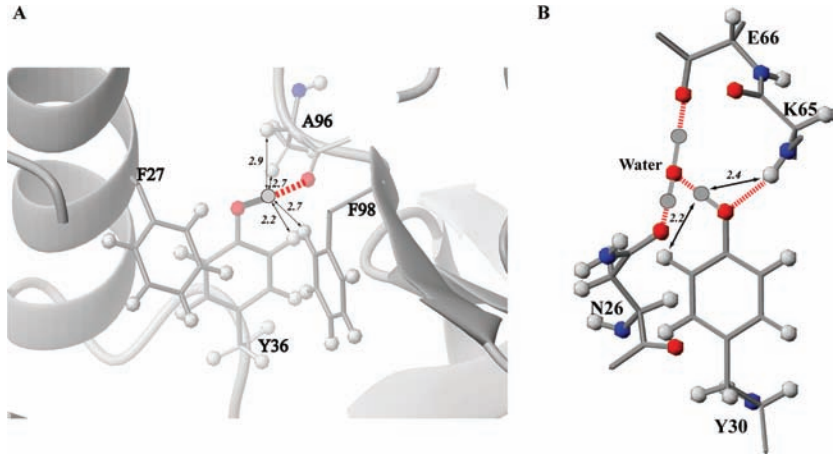

Figure 6. Hydrogen bonds involving the hydroxyl group of Tyr-36 (A) and Tyr-30 (B). Hydrogen, oxygen, and nitrogen atoms are depicted by white, red, and blue balls, respectively, and the deduced position of the hydroxyl hydrogen is depicted by gray balls. Experimentally observed NOEs involving the hydroxyl protons are depicted by the arrows, which are labeled with the distances in the crystal coordinates. The chemical shift values of the hydroxyl proton were 9.4 ppm for Tyr-36 and 9.5 ppm for Tyr-30. This structure is derived from the 2.1 Å crystal structure of EPPIb (PDB code 2NUL). This figure was produced by using the MolMol software.[55]

Δ_{nat} represent the observed and natural line widths, respectively, and k is the exchange rate.[14,15,44,46]

Conclusion

The hydrogen exchange study of Tyr hydroxyl protons using the deuterium isotope shift exerted on the $^{13}C_\zeta$ chemical shifts opens up various new possibilities for investigating protein structures and dynamics. The distribution in proteins and the fast intrinsic chemical exchange rates with surrounding water protons are peculiar features of the side chain hydroxyl groups, which distinguish them from the backbone amide groups.[2,4,12] Therefore information about the hydroxyl proton exchange rates obtained by the present approach is likely to yield complementary information on the dynamic aspects of protein structures obtained by various conventional methods. For example, comparisons between protein dynamics obtained by the aromatic ring flipping motions of phenylalanine and tyrosine residues[47−49] will be of considerable interest. The ring flipping of aromatic residues in the hydrophobic core region is concomitantly associated with the large amplitude breathing motion, which allows the rings to flip. Similar fluctuations, which occur on the millisecond to second time scale, are also required for proton−deuterium exchange phenomena for exchangeable groups in protein core regions. It is also interesting to measure the proton/deuterium fractionation factor of the side chain exchangeable groups in proteins using deuterium isotope shifts, since such analyses can potentially provide detailed information on the conformation and strength of the hydrogen bonds.[50−53]

In conclusion, we have presented a versatile and robust method for identifying Tyr residues with hydroxyl protons that slowly exchange with those of surrounding water molecules. Using (2*S*,3*R*)-[β_2,$\varepsilon_{1,2}$-$^2H_3$;0,α,β,ζ-$^{13}C_4$;^{15}N]-Tyr, ζ-SAIL Tyr, which has an optimal isotope-labeling design for the sequential NMR assignment and detection of $^{13}C_\zeta$ signals, we can apply the method for proteins larger than 40 kDa.[30,54] We are currently developing a similar approach to study the hydrogen−deuterium exchange rates for the hydroxyl groups in Ser and Thr residues in proteins. These studies will provide further information on auxiliary hydrogen bonds among side chain/side chain and side chain/backbone groups in solution, and ultimately yield accurate structures and dynamics.

Acknowledgment. This work was supported by the Targeted Protein Research Program (MEXT) to M.K. and by a Grant-in-Aid for Young Scientists (B) (21770110) to M.T. and Grant-in-Aid on Innovative Areas (4104) to J.J.

Supporting Information Available: Spectral simulations of the discrete ^{1}H NMR signal of the hydroxyl proton peak and the $^{13}C_\zeta$ signal in a H_2O/D_2O mixture at different hydrogen exchange rates; strips of the ^{13}C edited 3D NOESY-HSQC spectrum containing NOEs associated with the side chain hydroxyl proton of Tyr-36. This material is available free of charge via the Internet at http://pubs.acs.org.

JA907911Y

(46) Pople, J. A.; Schneider, W. G.; Bernstein, H. J. *High-Resolution Nuclear Magnetic Resonance*; McGraw-Hill: New York, 1959.
(47) Wüthrich, K.; Wagner, G. *FEBS Lett.* **1975**, *50*, 265–268.
(48) Wagner, G.; DeMarco, A.; Wüthrich, K. *Biophys. Struct. Mech.* **1976**, *2*, 139–158.
(49) Wagner, G.; Wüthrich, K. *Nature* **1978**, *275*, 247–248.
(50) Reuben, J. *J. Am. Chem. Soc.* **1986**, *108*, 1735–1738.
(51) Reuben, J. *J. Am. Chem. Soc.* **1987**, *109*, 316–321.
(52) Jarret, R. M.; Saunders, M. *J. Am. Chem. Soc.* **1985**, *107*, 2648–2654.
(53) Loh, S. N.; Markley, J. L. *Biochemistry* **1994**, *33*, 1029–1036.
(54) All of the isotopically labeled tyrosines used in this study are available from SAIL Technologies: http://www.sail-technologies.com/index.html.
(55) Koradi, R.; Billeter, M.; Wüthrich, K. *J. Mol. Graph.* **1996**, *14*, 51–55.